

BL16XU SUNBEAM ID

1. Introduction

BL16XU, which is referred to as SUNBEAM ID, together with its sister beamline BL16B2, was built to develop various industrial materials by utilizing the high-brightness beam at the large-scale synchrotron radiation facility in SPring-8. It is operated by the SUNBEAM Consortium, which is a private organization comprising 13 companies* (12 firms and one electric power group). BL16XU and BL16B2 began operations in September 1999, and

the beamline use contract was renewed in April 2018. In August 2020, we received an interim evaluation and obtained a "continuation" evaluation result.

X-rays emitted from an undulator are monochromatized, shaped, and converged in an optics hutch. The experimental hutch contains four experimental devices. Figure 1 and Table 1 schematically depict and outline the characteristics of BL16XU, respectively.

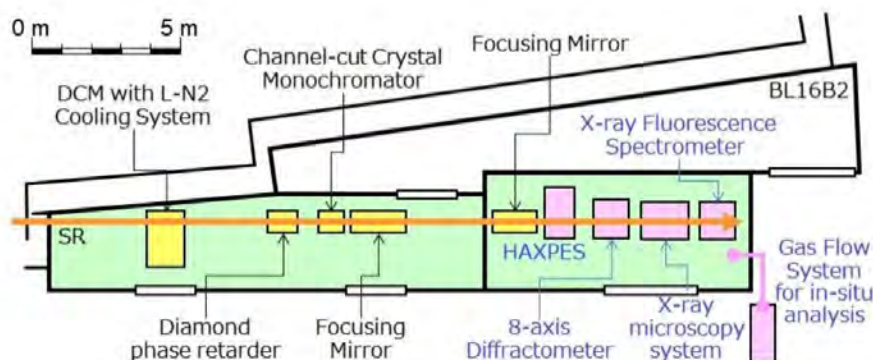


Fig. 1. Outline of BL16XU.

Table 1. Characteristics of BL16XU.

Light source	<i>In vacuo</i> X-ray undulator $\lambda = 40$ mm, $N = 112$
Energy range	4.5–40 keV
Energy resolution ($\Delta E/E$)	$\sim 10^{-4}$
Photon intensity, beam size	$\sim 10^{12}$ photons/s, < 1 mm \times 1 mm $\sim 10^{10}$ photons/s, < 500 nm \times 500 nm
Beam position stability	± 0.1 mm horizontal ± 0.8 mm vertical (5.0–30 keV)
Experimental facilities	HAXPES, XRD, XRF, Microbeam (Microscopy), Gas flow system (corrosive or toxic gas is possible)

*Kawasaki Heavy Industry, Ltd., Kobe Steel, Ltd., Sumitomo Electric Industries, Ltd., Sony Group Corp., Electric power group (Kansai Electric Power Co., Inc., Central Research Institute of Electric Power Industry), Toshiba Corp., Toyota

Central R&D Labs., Inc., Nichia Corp., Nissan Motor Co., Ltd., Panasonic Holdings Corp., Hitachi, Ltd., Fujitsu Ltd., Mitsubishi Electric Corp.

2. Utilization

Figure 2 shows the utilization of BL16XU in the past decade. The vertical axis shows the proportions of users, excluding the tuning and studying of the beamline itself. The upper graph depicts the utilization by field. The application fields are mainly semiconductors, batteries, and materials. In recent years, research related to green innovations, such as lithium-ion batteries, fuel cells, SiC, and GaN, has been progressing.

The lower graph shows the utilization of equipment (technology). The utilization of hard X-ray photoelectron spectroscopy (HAXPES) equipment, which was installed in 2014, is increasing. HAXPES is mainly used for semiconductors and battery materials.

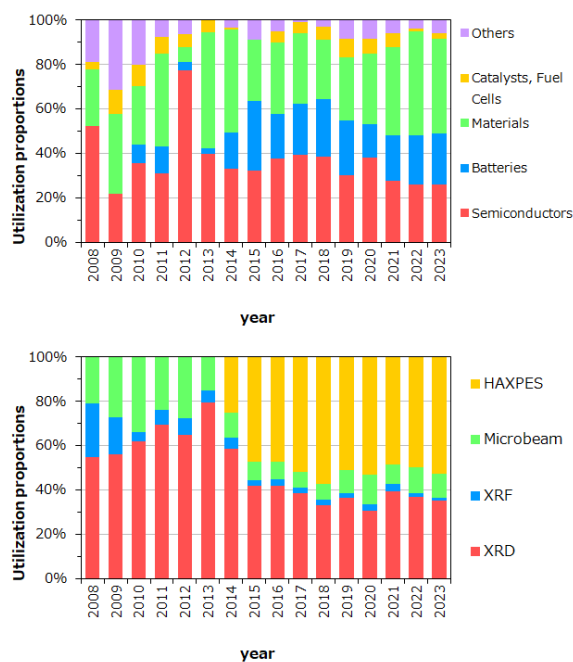


Fig. 2. Relative utilization times of BL16XU in the past decade.

3. Topics in FY2023

Below, the research and upgrades conducted in FY2023 are described.

3-1. Feasibility study on confocal X-ray diffraction with spiral slit at SUNBEAM

In FY 2018, a two-dimensional detector, the PILATUS 300K, which is made of CdTe elements of Dectris and is compatible with high-energy X-rays, and spiral slits that can obtain diffraction lines from deep within a sample (confocal position) were introduced at the same time. The spiral slits are designed to measure the diffracted X-rays from the confocal position in a Debye ring shape using a two-dimensional detector. These are planned for use in measuring stress from deep within a sample using high-energy X-rays with high penetration power and spiral slits. The width of the initially introduced spiral slit was 0.08 mm, and the results were reported in the 2019 annual report. The 0.15-mm-wide spiral slits were then added to improve the detection efficiency of diffracted signals. This is reported herein ^[1].

Figure 3 shows an overview of the spiral slits introduced into the SUNBEAM and set up for confocal X-ray diffraction. The spiral slits of the SUNBEAM are designed to produce confocal images with a scattering angle 2θ of 5° to 22° by processing spiral slits in a similar shape in two 1-mm-thick Ta plates of different sizes. By rotating the spiral slits one turn, the diffracted signals in this scattering angle range can pass through the spiral slits. The point at which X-rays passing through the incident slits and the diffraction lines passing through the two spiral slits intersect each other is the confocal point, and the design is such that only the diffracted signals at the confocal point can pass through. The gauge volume with a slit width of 0.15 mm was designed to be approximately one order of magnitude larger than that with a slit width of 0.08 mm, making it easier to obtain the diffraction

intensity.

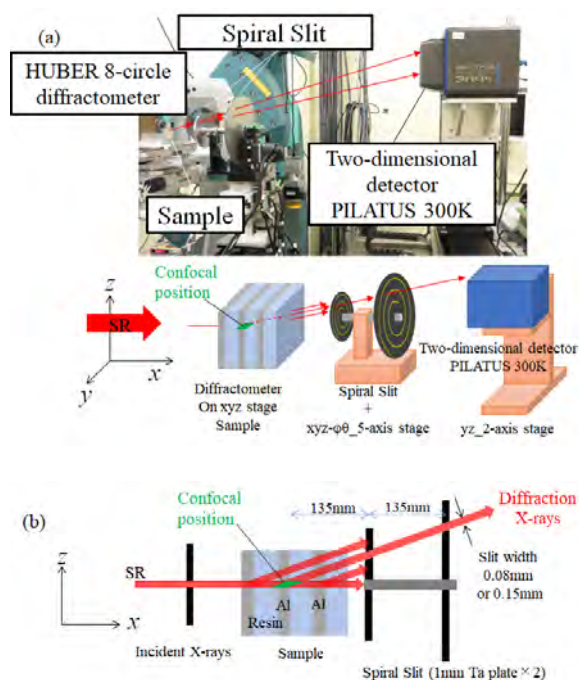


Fig. 3. (a) Photograph and overview of the experimental setup including the sample, the spiral slit, and the two-dimensional detector PILATUS 300K mounted on the two-axis stage. (b) Explanation of confocal X-ray diffraction using a spiral slit.

The experiment was carried out with a sample placed on the sample stage of the diffractometer at BL16XU with spiral slits downstream of the sample and a two-dimensional detector further downstream. The X-ray energy was spectrally resolved to 30 keV using a Si(111) surface spectrometer, and higher-order light was attenuated using a Rh-coated mirror at an incident angle of 1.5 mrad. The slit size for the incident X-rays was set equal to the slit width of each spiral slit. The spiral slit positions were fixed, and the two-dimensional detector, the PILATUS 300K, was placed with a camera length of approximately 800 mm. The two-dimensional detector, the PILATUS 300K with CdTe elements,

was placed on the yz two-axis stage. To evaluate stress distribution, the stress in the thickness direction of an Al plate during a bending test was evaluated using spiral slits with a slit width of 0.15 mm. Strain gauges were attached to both sides of a 2-mm-thick Al plate, and the imparted strain was measured. The diffraction pattern of Al(111) was measured while holding the imparted strain using a four-point bending jig so that the tensile and compressive strains were approximately 2.0×10^{-3} . With X-rays incident in the thickness direction, the center of the Al plate was determined from the intensity distribution within the ROI of Al(111), which was obtained by scanning the Al plate in the x-direction in a similar way to an evaluation of the spatial resolution. The stress distribution in the thickness direction was evaluated by scanning the sample in the x-direction within a range of ± 1.2 mm at intervals of 0.4 mm with respect to the center of the Al thickness. The measurement time at each point on the x-axis was approximately 15 min, including the scanning time of the two-dimensional detector. The stress was calculated using the $\cos^2\chi$ method.

As a result, although a low scattering angle is disadvantageous in terms of experimental accuracy because of a major change in stress with respect to the slope of $2\theta - \cos^2\chi$, the stress distribution changing from tension in the convex section of the Al plate to compression in the concave section of the Al plate because of the imparted bending is shown in Figure 4(a). Figure 4(b) shows the $2\theta - \cos^2\chi$ diagram for areas near both ends and at the center position of the Al plate. The result of the tensile test on an Al plate with a slit width of 0.08 mm showed a stress of 118 MPa with a strain of 2.0×10^{-3} [2]. On the other hand, with a slit width of 0.15

mm, the difference in stress between tension and compression was around 150 MPa, which was much greater, and the slope of the distribution became steeper. Therefore, in consideration of the confocal gauge size, the 0.15-mm-wide spiral slits can be effectively used in experiments that require diffraction intensity, such as in measurements of deep points.

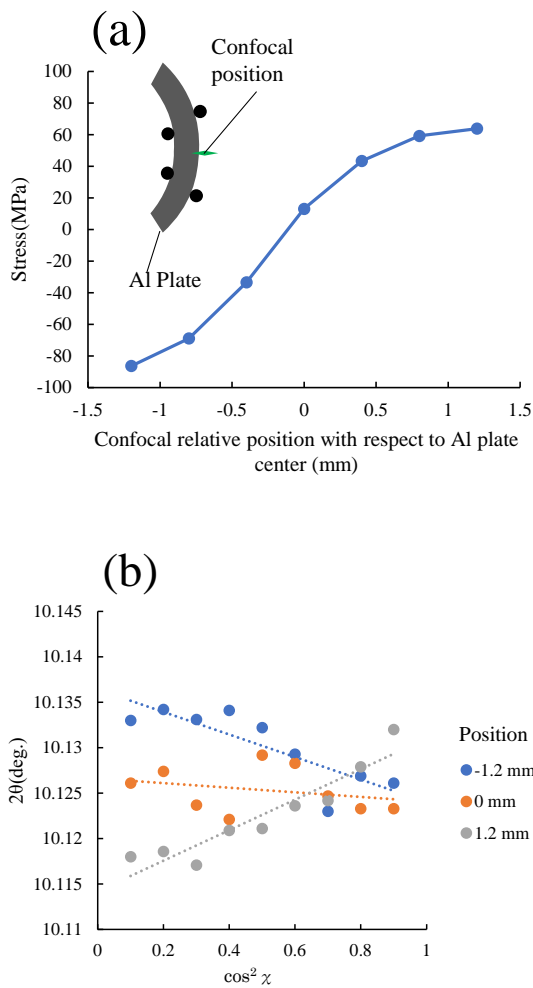


Fig. 4. Results of evaluating the stress distribution in an Al plate with a given bending strain of approximately 2.0×10^{-3} using spiral slits with a slit width of 0.15 mm. The negative side is tensile stress, whereas the positive side is compressive stress. (a) Relationship between the stress obtained from the $2\theta -$

$\cos^2\chi$ diagram and the confocal position of the Al plate. The inset is a conceptual diagram of the confocal point at -1.2 mm and the bent Al plate. (b) $2\theta - \cos^2\chi$ diagram of Al(111) at each scanning point on the x-axis.

MIWA Yasuo

SUNBEAM Consortium

Kawasaki Heavy Industries, Ltd.

References:

- [1] A. Kitahara et al., *SPring-8/SACLA Research Report* **11**, 419 (2023).
 [2] A. Kitahara et al., *SPring-8/SACLA Research Report* **9**, 554 (2021).